Carlo F. Barenghi
Yuri A. Sergeev
Editors

International Centre for Mechanical Sciences

Vortices and Turbulence at Very Low Temperatures

CISM Courses and Lectures, vol. 501

SpringerWienNewYork

SpringerWienNewYork

CISM COURSES AND LECTURES

The series presents lecture notes, monographs, edited works and proceedings in the field of Mechanics, Engineering, Computer Science and Applied Mathematics.
Purpose of the series is to make known in the international scientific and technical community results obtained in some of the activities organized by CISM, the International Centre for Mechanical Sciences.

INTERNATIONAL CENTRE FOR MECHANICAL SCIENCES

COURSES AND LECTURES - No. 501

VORTICES AND TURBULENCE AT VERY LOW TEMPERATURES

EDITED BY

CARLO F. BARENGHI
AND
YURI A. SERGEEV
NEWCASTLE UNIVERSITY, UK

SpringerWienNewYork

This volume contains 149 illustrations

Printed in Italy
SPIN 12325634

All contributions have been typeset by the authors.

ISBN 978-3-211-09446-4 SpringerWienNewYork

PREFACE

This book contains the lecture notes of the Advanced School "Vortices and Turbulence at Very Low Temperatures" organised at CISM, Udine, in July 2007. What motivated us in organising the school was the recent experimental and theoretical progress in the study of turbulence at very low temperatures near absolute zero using liquid and gaseous helium.

The aim of the school was to make more known to young turbulence researchers that the physical properties of helium allow experimenters to achieve extreme turbulence intensities, as measured by Rayleigh or Reynolds numbers. The second piece of information which we wanted to advertise is the observed striking similarity between ordinary turbulence and quantum turbulence (that is, turbulence in superfluid helium, in which the vortices are quantised). Quantum turbulence may thus represent a simplified version of the formidable turbulence problem.,

Why the need to advertise these results ? It is apparent that the problem of low temperature turbulence is at the intersection of physics communities which, normally, would not normally communicate much with each other: fluid dynamicists (who better understand the aspects of turbulence), low temperature physicists (who know the techniques to handle liquid helium) and atomic physicists (who can create quantised vortices in ultra-cold, Bose-Einstein condensed atomic gases). The school which we organised was thus an attempt to lower barriers between disciplines and stimulate young researchers with different backgrounds.

We are grateful to our colleagues Natalia Berloff, Shaun Fisher, Joe Niemela and Ladik Skrbek who gave the lectures on vortices and

low temperature turbulence collected in this book. We are indebted to Professor Katepalli Sreenivasan who gave an exciting presentation of new experimental techniques to visualise liquid helium. We would like to thank CISM for hosting this event, in particular Cara Toros and the staff who helped with the day-to-day organization, Professor Paolo Serafini for the editorial activity, and CISM's Rector Professor Giulio Maier. Finally, we are grateful to Professor Alfredo Soldati for encouraging us in pursuing the idea of this advanced school.

Carlo Barenghi and Yuri Sergeev
Newcastle University
Newcastle upon Tyne, UK
January 2008

CONTENTS

Introduction to quantised vortices and turbulence

Carlo F. Barenghi*

School of Mathematics and Statistics, Newcastle University,
Newcastle upon Tyne, U.K.

Abstract This chapter contains an introduction to liquid helium, the two–fluid model, quantised vortices and quantum turbulence. The last section gives a flavour of current research on quantum turbulence. At the end of the chapter a number of exercises test the reader's own understanding.

1 Liquid helium

1.1 The race toward absolute zero

During the XIX century physicists developed the science of thermodynamics and understood that there is a limit to the degree of cold which is possible. The temperature scale which starts from this limit is called the Kelvin scale of temperatures. One Kelvin degree is equal to one degree on the usual Centigrade scale, and absolute zero, $T = 0$ K, corresponds to $T = -273.15$ C. Physicists found that if the temperature is reduced there is less thermal disorder, thus the fundamental properties of matter become more apparent. Low temperature physics laboratories competed against each other, racing toward absolute zero, and attempted to liquefy all known gases, thus cooling matter to lower and lower temperatures. Oxygen become liquid at $T = 90$ K. Nitrogen required 77 K. In 1898 Dewar succeeded in liquefying hydrogen at $T = 20$ K. The only gas which resisted being liquefied was helium. Although helium is the second most common element in the Universe, it was identified only in the XIX century, first in the spectrum of solar radiation and then, by Ramsay, in rocks containing

*I am grateful to CISM for organizing the Advanced School on Vortices and Turbulence at Low Temperatures and for supporting the publication of these lecture notes. I also wish to thank Professor Alfredo Soldati for encouraging this Advanced School, and to Professor Yuri Sergeev for reading my manuscript. I also acknowedge the support of EPSRC, grants GR/T08876/01 and EP/D040892/1.

uranium. It was only in 1908 that Onnes succeeded in creating the first sample of liquid helium at $T = 4$ K. Few years later, in 1911, Onnes discovered superconductivity, the ability of some metals (e.g. mercury, tin, lead) and alloys to sustain electrical currents without any electrical resistance.

1.2 Engineering applications

Today the main practical application of liquid helium is cryogenic cooling. If we want to measure the low temperature properties of a substance (e.g. the specific heat or the thermal conductivity) it is necessary to cool a sample of that substance; the best way to extract heat it from the sample is to immerse it into a liquid, so that the area of thermal contact is maximised. At temperatures of few Kelvin degrees, the only existing liquid is helium: any other substance is solid.

A common application of helium is cooling superconducting magnets. The coils of these magnets are made of alloys which become superconducting if the temperature is less than a critical value. Superconducting magnets are routinely used in hospitals to make scans. They are also used in high energy physics laboratories to accelerate beams of elementary particles. An example is CERN's Large Hadron Collider. Along the 27 km long ring of the LHC there are more than one thousand superconducting magnets; to provide a magnetic field strength of $80,000$ Gauss, each magnet is held at the operating temperature of $T = 1.8$ K. Liquid helium is also used by astrophysicists to cool infrared detectors; for example, the IRAS satellite carried 720 litres of liquid helium held at $T = 1.6$ K.

1.3 Helium I and helium II

Figure 1.3.1 shows the typical phase diagram (pressure versus temperature) of an ordinary substance. In the diagram, the triple point marks the co-existence of gas, liquid and solid phases. The first experiments which investigated the properties of liquid helium were performed by Onnes and Dana in Leiden. Onnes and Dana found that liquid helium is transparent and has density equal to approximately 1/6 of water's. They also noticed that, upon cooling the liquid helium by pumping on its vapour, the bubbling ceased when helium's temperature dropped below a critical value of approximately 2 K. Motivated by this strange effect, which suggests that some physical transformation takes place, Onnes and Dana measured helium's specific heat, C. They found that the temperature dependence of C has a remarkable peak at the same critical temperature 2 K. From the shape of the specific heat curve, they called T_λ this critical temperature. The value of T_λ on the current temperature scale is $T_\lambda = 2.1768$ K at

saturated vapour pressure (SVP).

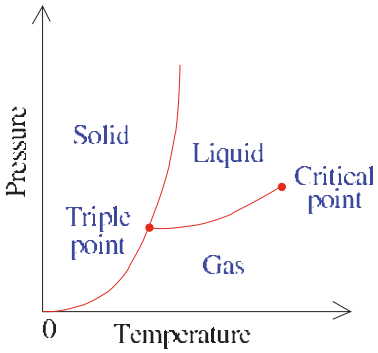

Figure 1.3.1. Phase diagram of an ordinary substance.

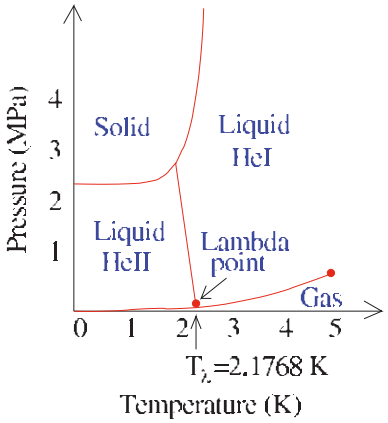

Figure 1.3.2. Phase diagram of liquid helium.

Soon it became clear that the properties of liquid helium above and below T_λ are very different. The low temperature liquid phase of helium was called helium II to distinguish it from the high temperature liquid phase called helium I. Figure 1.3.2 shows the phase diagram of liquid helium. Note the absence of a triple point and the fact that helium remains liquid down to absolute zero. To obtain solid helium, a pressure of about 25 bars must be applied. The boundary between helium I and helium II is called the lambda line; the intersection of the lambda line with the saturated pressure curve (along which most experiments are performed) is the lambda point.

The most striking property of helium II is superfluidity, which is the ability to flow without any viscous dissipation. Superfluidity was discovered independently by Kapitza and Allen in 1938, for which Kapitza was awarded the Nobel prize. Following the discovery of superfluidity, further experiments revealed that the flow of helium II has more strange properties if compared to the flow of ordinary liquids (including helium I). It was only in the 1940's that Landau and Tisza developed a theory, called the two–fluid model, which accounts for the observed flow of helium II, at least at small velocities. Landau was awarded the Nobel prize for his work on superfluidity. A prediction of the two–fluid model was an unusual mode of oscillation called second sound, which was observed by Peshkov in 1941.

In the 1940's, experiments on the rotational motion of helium II revealed more surprises. The quantisation of the circulation, predicted by Onsager (1948) and Feynman (1955), both Nobel prize winners, explained these experiments. The quantum of circulation was first observed by Vinen in 1961. Vinen also performed the first experimental investigations of quantum turbulence. Quantum turbulence limits the otherwise ideal properties of helium II to transfer heat, so it is important in the engineering applications of liquid helium. Current research in helium II is concerned with the similarities and difference between classical turbulence and quantum turbulence.

1.4 ^{4}He and ^{3}He

The nucleus of ordinary helium (^{4}He) consists of two protons and two neutrons. Naturally occurring helium gas contains a small fraction (approximately 1 part in 10^7) of the rare isotope ^{3}He, whose nucleus contains only one neutron. In 1972 Richardson, Lee and Osheroff were awarded the Nobel prize for the discovery that pure liquid ^{3}He becomes superfluid too, but at much colder temperatures (of the order of few milliKelvins) than ^{4}He.

1.5 Bose–Einstein condensation

The fundamental physical mechanism which is responsible for superfluidity is Bose – Einstein condensation (BEC), see Pethick and Smith (2001). Here it suffices to say that, according to quantum mechanics, a particle has also a characteristic wavelength, λ, associated with its momentum, p. In an ordinary gas, λ is much smaller than the average separation between the atoms, d. If the temperature is reduced, λ increases. At some critical temperature T_c, λ becomes of the order of d. In 1924 Bose and Einstein considered a sistem of bosons (particles with integer spin) and realized that, if the system consists of bosons, at this critical temperature it undergoes a

phase transition, which corresponds to condensation in momentum phase. It was only in 1938 that London noticed that BEC is relevant to the superfluidity of liquid helium.

In the case of ^{3}He, the nucleus is not a boson (it has semi–integer spin), but paired atoms form Cooper pairs which are bosons and undergo BEC.

The study of BEC was greatly boosted by Wiemann, Cornell and Ketterlee's. They discovered BEC in trapped, ultra–cold alkali atoms in 1995, for which they were awarded the Nobel prize.

2 Two–fluid model

2.1 Thermal and mechanical effects

Early experiments showed that the motion of helium II has unusual properties. For example, consider a vessel A which contains helium and is linked to the helium in the bath B via a superleak S, as in Figure 2.1.1 left. A superleak is a very small hole (or holes); it can be realized, for example, by filling a channel with very fine powder, so fine that any ordinary fluid could not go through it. It was found that heating the helium in A with a resistor induces not only a temperature difference $\Delta T = T_A - T_B$, but also a flow from B to A through the superleak S, hence a pressure difference Δp, which is proportional to the height difference between the liquid in A and the liquid in B. This pressure difference can be large enough to create a small fountain, if A is open at the top (fountain effect). Note that the velocity (into A) opposes the flow of entropy (out of A), unlike what happens in an ordinary fluid.

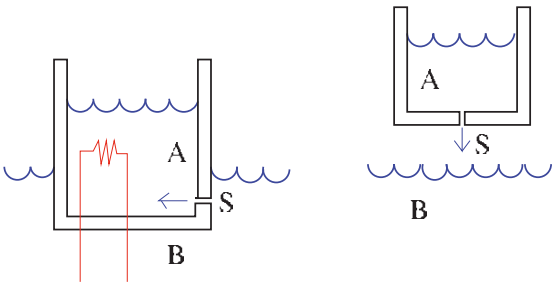

Figure 2.1.1. Left: thermo–mechanical effect. Right: mechano–thermal effect.

A second unusual effect, discovered by Daunt and Mendelsson and shown in Figure 2.1.1 right, is the following. If the vessel A is lifted above the bath B and helium flows out of the superleak S, the temperature in A increases,

whereas the temperature is B decreases. This phenomenon is called the mechano–caloric effect.

Careful measurements by Kapitza of the chemical potential μ revealed that in these experiments μ remains the same in A and B: $\mu(p_A, T_A) = \mu(p_B, T_B)$. Since $d\mu = -sdT + dp/\rho$, where s is the specific entropy, we conclude that

$$\Delta p = \rho s \Delta T, \tag{2.1.1}$$

In another set of experiments it was found that helium's viscosity, η, seems to change at $T < T_\lambda$, depending on how it is measured.

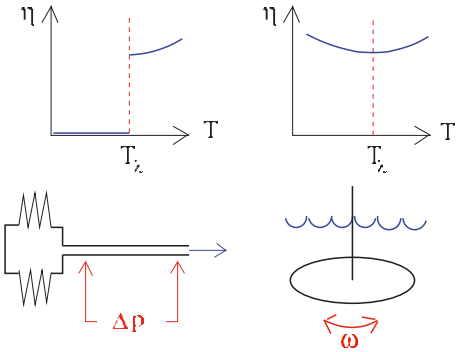

Figure 2.1.2. Left: the viscosity η, determined from the measurement of the pressure drop in a thin pipe, is discontinuous when plotted versus the temperature T. Right: if η is determined from the damping of an oscillating disk, it is continuous with T.

If the viscosity is measured by pushing helium along a capillary using bellows and detecting the pressure gradient along the channel, then $\eta = 0$ within experimental accuracy (see Figure 2.1.2 left). If the viscosity is measured by observing the damping of an oscillating disk, then $\eta \neq 0$ (see Figure 2.1.2 right).

2.2 Landau's equations

The apparently paradoxical results described in the previous subsection are explained by the two-fluid model of Landau and Tisza, see Landau and Lifshitz (1987) and Donnelly (1991). In this model, helium II is described as the intimate mixture of two fluids: the superfluid and the normal fluid. The first is related to the quantum ground state, and has zero viscosity

and entropy. The second consists of thermal excitations and carries the total viscosity and entropy of the liquid. Each fluid has its own velocity and density fields, $\mathbf{v}_s$ and ρ_s for the superfluid and $\mathbf{v}_n$ and ρ_n for the normal fluid; the total density of helium II, $\rho = \rho_n + \rho_s$, is approximately temperature independent. The table below summarises the two–fluid model:

component	velocity	density	viscosity	entropy
normal fluid	$\mathbf{v}_n$	ρ_n	η	s
superfluid	$\mathbf{v}_s$	ρ_s	0	0

The two–fluid model accounts for the experimental observations. The superleak S is so small that the viscous normal fluid cannot move through it: only the superfluid flows through S. The observation that the chemical potential is constant across S both in the steady state (when $\mathbf{v}_s = 0$ in the superleak) and during transients (when $\mathbf{v}_s \neq 0$) led Landau to postulate that gradients of the chemical potential are responsible for the acceleration of the superfluid.

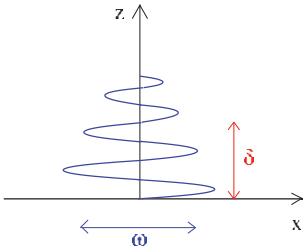

Figure 2.2.1. Penetration depth.

The relative proportion of superfluid and normal fluid at a given temperature was determined by Adronikashvili. He used the fact that the motion of an oscillating boundary penetrates into a viscous fluid only a distance of the order of $\sqrt{2\nu/\omega}$, where $\nu = \eta/\rho$, ν is the kinematic viscosity, η the viscosity, and ω the angular frequency of the oscillation - see Figure 2.2.1.

Adronikashvili's apparatus, shown schematically in Figure 2.2.2, was a special pendulum which consisted of a suspended stack of disks. Let Δz be the distance between the disks. If $\Delta z \ll \delta = \sqrt{2\eta/(\rho_n\omega)}$ the normal fluid is trapped between the disks and contributes to the moment of inertia of the pendulum, whereas the superfluid does not contribute (being inviscid,

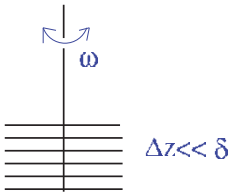

Figure 2.2.2. Adronikashvili's pendulum.

it moves freely between the disks). By measuring the damping rate of the torsional oscillations, Adronikashvili determined the ratios ρ_s/ρ and ρ_n/ρ as functions of the temperature T, which are shown schematically in Figure 2.2.3. Note that if the temperature is reduced the normal fluid fraction ρ_n/ρ decreases rapidly; below $T \approx 0.7$ K the normal fluid can be neglected.

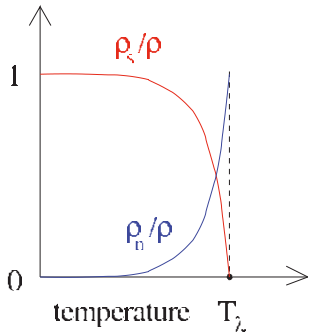

Figure 2.2.3.

The mathematical formulation of the two–fluid model consists of the equations of mass and entrophy conservation, and the equations of momentum conservation of the normal fluid and the superfluid, respectively. These equations are

$$\frac{\partial \rho}{\partial t} + \nabla \cdot (\rho_n \mathbf{v}_n + \rho_s \mathbf{v}_s) = 0, \tag{2.2.1}$$

$$\frac{\partial (\rho s)}{\partial t} + \nabla \cdot (\rho s \mathbf{v}_n) = 0, \tag{2.2.2}$$

$$\frac{\partial \mathbf{v}_n}{\partial t} + (\mathbf{v}_n \cdot \nabla)\mathbf{v}_n = -\frac{1}{\rho}\nabla p - \frac{\rho_s}{\rho_n} s \nabla T + \frac{\eta}{\rho_n}\nabla^2 \mathbf{v}_n, \tag{2.2.3}$$

$$\frac{\partial \mathbf{v}_s}{\partial t} + (\mathbf{v}_s \cdot \nabla)\mathbf{v}_s = -\frac{1}{\rho}\nabla p + s\nabla T. \tag{2.2.4}$$

Equation 2.2.2 states that entropy flows with the normal fluid. Note that, in isothermal conditions, the superfluid obeys the classical Euler equation, and the normal fluid obeys the classical Navier–Stokes equation.
Finally Landau recognised that, since $\mathbf{v}_s$ is proportional to the gradient of the phase of a quantum mechanical wavefunction, we must also have

$$\nabla \times \mathbf{v}_s = 0. \tag{2.2.5}$$

It must be stressed that Equation (2.2.3) and (2.2.4) are valid only at small velocities. In the presence of quantised vortices Landau's equation require modifications.

2.3 The spectrum of elementary excitations

The normal fluid consists of thermal excitations of energy ϵ and momentum $\mathbf{p}$. Landau showed that the shape of the dispersion curve $\epsilon = \epsilon(p)$, where $p = |\mathbf{p}|$, is responsible for the superfluid nature of helium II. Landau's spectrum, confirmed by neutron scattering experiments, is shown in Figure 2.3.1. Note the minimum at momentum p_0 and energy Δ. The excitations at low p (linear part of the spectrum) are called phonons; the excitations in the quadratic region near the minimum of the dispersion curve are called rotons.

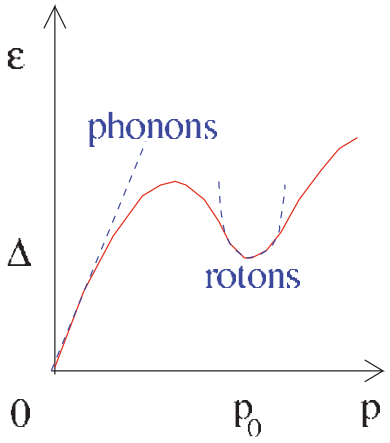

Figure 2.3.1. Landau's spectrum of the excitations. Note the roton minimum at (p_0, Δ_0).

Landau's argument for superfluidity is the following. Consider an object (e.g. an ion) of mass m moving with momentum $\mathbf{p}_1 = mV_1$ and energy E_1 which creates an excitation of energy ϵ and momentum $\mathbf{p}$ changing its own energy and momentum to E_2 and $\mathbf{p}_2$. Conservation of energy and momentum requires $E_1 = E_2 + \epsilon$ and $\mathbf{p}_1 = \mathbf{p}_2 + \mathbf{p}$, hence

$$P_1 p \cos\theta = m\epsilon + \frac{1}{2}p^2, \tag{2.3.1}$$

where θ is the angle between $\mathbf{p}_1$ and $\mathbf{p}$. Thus the object can lose energy and create an excitation if the initial velocity satisfies

$$V_1 > \frac{p}{2m} + \frac{\epsilon}{p} \approx \frac{\epsilon}{p}. \tag{2.3.2}$$

Let us minimise this velocity ϵ/p:

$$\frac{d}{dp}\left(\frac{\epsilon}{p}\right) = -\frac{1}{p^2}\epsilon + \frac{1}{p}\frac{d\epsilon}{dp} = 0. \tag{2.3.3}$$

We find:

$$\frac{d\epsilon}{dp} = \frac{\epsilon}{p}. \tag{2.3.4}$$

The minimum of ϵ/p thus corresponds to the line from the origin to a point slightly to the right of (p_0, Δ) on the dispersion curve; the critical velocity is $V_1 = V_c = 58$ m/s (at SVP). In conclusion, at sufficiently low temperature such that the normal fluid is negligible, we expect the ion to experience no drag for $0 < V_1 < V_c$.

At SVP, an ion moving in liquid helium creates a vortex ring at velocity smaller than V_c. Fortunately, at higher pressures the velocity of roton creation is smaller than the velocity required to create a vortex ring, and Landau's argument can be tested directly, as done by Allum *et al.* (1977).

3 Consequences of the two–fluid model

3.1 Second sound

The existence of two separate fluid components has a striking consequence on the oscillatory motion of helium II. Let us consider helium at rest ($\mathbf{v}_{n0} = 0$, $\mathbf{v}_{s0} = 0$) with density $\rho_0 = \rho_{s0} + \rho_{n0}$, pressure p_0, temperature T_0 and entropy s_0. We introduce small perturbations (indicated by primed quantities) $\rho = \rho_0 + \rho'$, $\rho_n = \rho_{n0} + \rho_n'$, $\rho_s = \rho_{s0} + \rho_s$, $\mathbf{v}_n = \mathbf{v}_n'$, $\mathbf{v}_s = \mathbf{v}_s'$, $p = p_0 + p'$, $T = T_0 + T'$ and $s = s_0 + s'$; neglecting quadratic terms in the perturbations, Landau's equations become

$$\frac{\partial \rho'}{\partial t} + \rho_{n0} \nabla \cdot \mathbf{v}'_n + \rho_{s0} \nabla \cdot \mathbf{v}'_s = 0, \tag{3.1.1}$$

$$\rho_0 \frac{\partial s'}{\partial t} + s_0 \frac{\partial \rho'}{\partial t} + \rho_0 s_0 \nabla \cdot \mathbf{v}'_n = 0, \tag{3.1.2}$$

$$\frac{\partial \mathbf{v}'_n}{\partial t} = -\frac{1}{\rho_0} \nabla p' - \frac{\rho_{s0}}{\rho_{n0}} s_0 \nabla T', \tag{3.1.3}$$

$$\frac{\partial \mathbf{v}'_s}{\partial t} = -\frac{1}{\rho_0} \nabla p' + \rho_{s0} s_0 \nabla T'. \tag{3.1.4}$$

In writing these equations we have neglected the viscous term $\eta \nabla^2 v_{\rm n}$, because we know already that its effect is to damp any motion. Assuming the solution in the form $e^{i\omega(t-x/c)}$, we find two values for the phase speed c:

$$c_1 = \sqrt{\left(\frac{\partial p}{\partial \rho}\right)_0}, \tag{3.1.5}$$

$$c_2 = \sqrt{\frac{\rho_{s0} s_0^2 T_0}{\rho_{n0} C_V}}. \tag{3.1.6}$$

We conclude that there are two modes of oscillation. The first mode is a pressure and density wave at (almost) constant temperature and entropy, in which $\mathbf{v}_n$ and $\mathbf{v}_s$ move in phase. In analogy with ordinary sound, we call this mode first sound. The second mode is a temperature and entropy wave at (almost) constant pressure and density, in which $\mathbf{v}_n$ and $\mathbf{v}_s$ move in anti–phase. We call this mode second sound. The speed of first sound is $c_1 \approx 200$ m/s at all temperatures; the speed of second sound, c_2, is approximately ten times less, and drops to zero as $T \to T_\lambda$.

It is interesting to notice that in second sound temperature perturbations obey the wave equation

$$\frac{\partial^2 T'}{\partial t^2} \approx c_2^2 \nabla^2 T',$$

whereas in ordinary fluids (e.g. helium I) they obey the heat equation

$$\frac{\partial T'}{\partial t} = \kappa \nabla^2 T'.$$

3.2 Thermal counterflow

Another consequence of the existence of two fluids is the unusual form of heat transfer. Consider Figure 3.2.1. A closed channel is open to the helium bath at one end; a resistor, placed at the closed end, dissipates a known heat flux $\dot{Q}$. This heat flux is carried away by the normal fluid, $v_n = \dot{Q}/(\rho ST)$. With the channel being closed, the mass flux is zero, $\rho_n v_n + \rho_s v_s = 0$, hence the superfluid moves towards the resistor, $v_s = (\rho_n/\rho_s)v_n$, setting up a counterflow velocity $v_{ns} = v_n - v_s$ which is proportional to the applied heat flux:

$$v_{ns} = v_n - v_s = \frac{\dot{Q}}{\rho_s ST}. \tag{3.2.1}$$

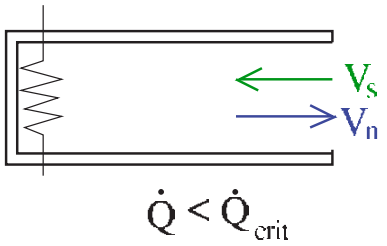

Figure 3.2.1. Laminar counterflow for $\dot{Q} < \dot{Q}_{crit}$.

Provided that $\dot{Q}$ is less than a critical heat flux $\dot{Q}_c$, this form of heat transfer is laminar.

4 Quantised vortex lines

4.1 Helium in rotation

Quantum mechanics introduces remarkable constraints on the rotational motion of helium II. It is instructive to consider the rotation of an ordinary, classical fluid first. A bucket of water which rotates at constant angular velocity Ω around the z axis has a height profile given by

$$z = \frac{\Omega^2 r^2}{2g}, \tag{4.1.1}$$

as shown in Figure 4.1.1 left; the water's velocity field is $\mathbf{v} = \Omega\hat{\boldsymbol{\phi}}$ (solid body rotation), and the vorticity is $\boldsymbol{\omega} = \nabla \times \mathbf{v} = 2\Omega\hat{\mathbf{z}}$, where $\hat{\mathbf{z}}$ and $\hat{\boldsymbol{\phi}}$ are the unit vectors along the axial and azimuthal direction respectively.

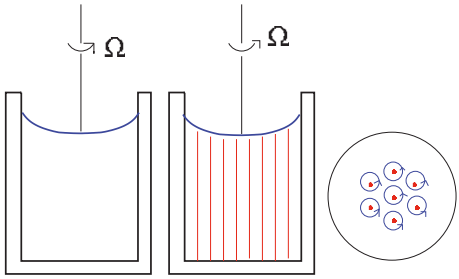

Figure 4.1.1. Left: classical fluid in rotation. Middle: rotating helium II. Right: top view of the vortex lattice.

The rotation of helium II is very different, because quantum mechanics introduces important constraints on the rotational motion. According to the two–fluid model, $\nabla \times \mathbf{v}_s = 0$, which means that the superfluid component cannot rotate; we expect that the profile of rotating helium II is

$$z = \left(\frac{\rho_n}{\rho}\right) \frac{\Omega^2 r^2}{2g}. \tag{4.1.2}$$

which is temperature dependent.

The observed profile did not agree with this prediction. The puzzle was solved by Onsager (1949) and Feynman (1955), who argued that the superfluid forms vortex lines, as in Figure 4.1.1 middle and right, around which the circulation κ is quantised, see Donnelly (1991):

$$\oint_C \mathbf{v}_s \cdot \mathbf{d}\boldsymbol{\ell} = \kappa, \tag{4.1.3}$$

where h is Planck's constant. The quantum of circulation (measured by Vinen in 1961) is

$$\kappa = \frac{h}{m} = 9.97 \times 10^{-4}\ cm^2\ s^{-1}, \tag{4.1.4}$$

where m is the mass of the helium atom.

Equation 4.1.3 can be used to determine the velocity field. Let C be a circle of radius r around the axis of the vortex; then the superfluid velocity is

$$v_\phi = \frac{\kappa}{2\pi r}, \tag{4.1.5}$$

as shown in Figure 4.1.3.

In Section 5 we shall see that the vortex core is hollow, so Equation 4.1.5 is valid only for $r \geq a_0$ where a_0 is the vortex core radius.

Figure 4.1.2. Vortex line

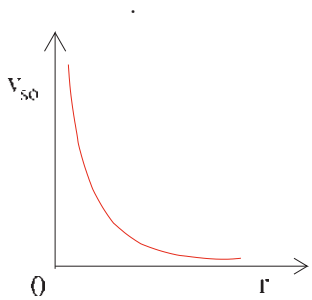

Figure 4.1.3. Velocity field around a vortex line.

4.2 The first vortex

The critical angular velocity Ω_c for the appearance of the first vortex line can be determined in the following way, see Donnelly (1991). Thermodynamical equilibrium requires minimisation of the free energy, $F = E - TS$, in the rotating frame of reference, which is

$$F' = F - \mathbf{\Omega} \cdot \mathbf{L} = (E - TS - \mathbf{\Omega} \cdot \mathbf{L}, \tag{4.2.1}$$

where E is internal energy, $\mathbf{\Omega}$ the angular velocity, and $\mathbf{L}$ the angular momentum. Let $T = 0$ and consider helium II contained in a rotating cylinder of radius R. The first vortex appears if

$$\Delta F' = F'_{vortex} - F'_{no\ vortex} = E - \Omega L < 0, \tag{4.2.2}$$

where the energy and the angular momentum (per unit length) are

$$E = \int_0^{2\pi} d\phi \int_{a_0}^{R} \frac{\rho_s v_s^2}{2} r dr, \tag{4.2.3}$$

$$L = \int_0^{2\pi} d\phi \int_{a_0}^{R} \rho_s r v_s r dr. \tag{4.2.4}$$

Substituting $v_s = \kappa/(2\pi r)$ we find that the critical velocity of vortex appearance is

$$\Omega_c = \frac{\kappa}{2\pi R^2} \ln (R/a_0), \tag{4.2.5}$$

where $a_0 \approx 10^{-8}$ cm is the vortex core radius.

4.3 Vortex lattice

If Ω is increased past Ω_c, more and more vortex lines appear in the flow. A bucket of helium rotating at constant angular velocity $\Omega > \Omega_c$ contains a lattice of quantised vortex lines aligned along the axis of rotation as shown in Figure 4.1.1. The lattice is steady in the rotating frame (see Figure 4.1.1 right; the number of vortex lines per unit area is given by Feynman's rule

$$n = \frac{2\Omega}{\kappa}. \tag{4.3.1}$$

Note that although the microscopic superflow is potential ($v_s \sim 1/r$), the macroscopically–averaged flow which results from the vortex lattice corresponds to solid body rotation ($v_s \sim \Omega r$). In other words, by creating n quantised vortices per unit area, helium II has the same (large–scale) vorticity of a classical rotating fluid ($2\Omega = n\kappa$).

Equation (4.3.1) has been tested by direct visualisation of quantised vortices at low temperatures by citeWP74; their technique consisted in trapping electrons along the vortex lines and then collecting them on electrodes at the top of the container. More recently, direct visualisation of quantised vorticity was achieved by Bewley, Lathrop, and Sreenivasan (2006), who trapped micron–size particles in the vortices and imaged the particles with a laser. The method, called Particle Image Velocimetry (PIV), is described in the Chapter by Sergeev in this book. Quantised vorticity in atomic Bose–Einstein condensates has also been achieved directly using lasers, see Madison, Chevy, Wohlleben, and Dalibard (2000).

5 The Bose–Einstein condensate model

5.1 The NLSE

The natural question raised by Equation (4.1.5) is: what happens if $r \to 0$? To answer this question we need a model for the vortex core.

Such model is provided by the Nonlinear Schrödinger Equation (NLSE), also called the Gross–Pitaevskii (GP) equation (see the Chapter by Berloff in this book). The NLSE describes accurately weakly interacting Bose particles in atomic Bose–Einstein condensates, In the case of helium II, the interaction between the bosons is strong, and our core model will be only qualitative, but sufficient for our purpose.

In the Hartree approximation, a condensate of weakly interacting Bose particles is described by a single particle wavefunction ψ for N bosons of mass m which obeys the NLSE

$$i\hbar\frac{\partial\psi}{\partial t} = -\frac{\hbar^2}{2m}\nabla^2\psi + V_0|\psi|^2\psi - E_0\psi. \tag{5.1.1}$$

where V_0 is the strength of the repulsive interaction between the bosons and E_0 is the energy increase upon adding one boson (chemical potential).

The simplest solution of Equation (5.1.1) is the uniform condensate at rest:

$$\psi = \psi_\infty = \sqrt{\frac{E_0}{V_0}}, \tag{5.1.2}$$

Another exact solution is the 1–dimensional solution in $0 \le x < \infty$ near a wall at $x = 0$:

$$\psi = \psi_\infty = \tanh(x/a_0), \tag{5.1.3}$$

where the quantity

$$a_0 = \sqrt{\frac{\hbar^2}{mE_0}} \tag{5.1.4}$$

is called the healing length.

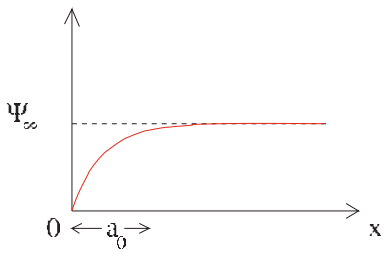

Figure 5.1.1. Condensate near the wall. The healing length is a_0.

It is easy to verify that small perturbations of the uniform solution obey the dispersion relation

$$\omega = k\sqrt{\frac{E_0}{m}\left(1 + \frac{\hbar^2 k^2}{4mE_0}\right)} \tag{5.1.5}$$

shown in Figure 5.1.2, where ω is the angular frequency and k is the wavenumber. Note that, if $k \ll 1$, then $\omega \approx ck$ where $c = \sqrt{E_0/m}$ is the speed of sound; if $k \gg 1$, then $\omega \approx \hbar^2 k^2/(2m)$, which is the dispersion relation of free particles. Note also that the NLSE dispersion relation – see Figure 5.1.2 – does not have a roton minimum like Landau's spectrum – see Figure 2.3.1.

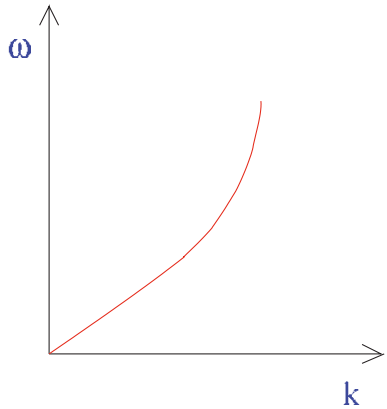

Figure 5.1.2. NLSE: dispersion relation $\omega = \omega(k)$.

5.2 Fluid dynamics interpretation of the NLSE

The Madelung transformation

$$\psi = Re^{iS}, \tag{5.2.1}$$

where R is the amplitude and S is the phase of ψ, provides us with a simple fluid dynamics interpretation of the NLSE. If we substitute Equation (5.2.1) into Equation (5.1.1), we obtain the continuity equation

$$\frac{\partial \rho_s}{\partial t} + \nabla \cdot (\rho_s \mathbf{v}_s) = 0 \tag{5.2.2}$$

and the (quasi) Euler equation

$$\rho_s \left(\frac{\partial v_{sj}}{\partial t} + v_{sk} \frac{\partial v_{sj}}{\partial x_k} \right) = -\frac{\partial p}{\partial x_j} + \frac{\partial \Sigma_{jk}}{\partial x_k} \tag{5.2.3}$$

where the usual convention applies of summation over repeated indices,

$$\rho_s = mR^2 \tag{5.2.4}$$

is the density,

$$\mathbf{v}_s = \frac{\hbar}{m} \nabla S \tag{5.2.5}$$

is the velocity (with Cartesian components v_{sk}, $k = 1, 2, 3$),

$$p = \frac{V_0}{2m^2} \rho_s^2 \tag{5.2.6}$$

is the pressure, and

$$\Sigma_{jk} = \left(\frac{\hbar}{2m} \right)^2 \rho_s \frac{\partial^2 \ln \rho_s}{\partial x_j \partial x_k} \tag{5.2.7}$$

is the quantum stress. Note that, without the quantum stress, the NLSE would describe a classical inviscid Euler fluid.

5.3 Vortex line solution of the NLSE

A vortex line solution of the NLSE is easily found. We use cylindrical coordinates (r, ϕ, z), substitute $S = \phi$ into $\psi = Re^{iS}$, and solve for the resulting velocity and density fields. We obtain

$$\mathbf{v}_s = \frac{\hbar}{m} \nabla S = \frac{\kappa}{2\pi r} \hat{\boldsymbol{\phi}}, \tag{5.3.1}$$

which is the velocity field of a vortex line aligned along z shown in Figure 4.1.3.

To find the density field corresponding to this velocity field a numerical integration is required; the result is very similar to what shown in Figure 5.1.1: the density drops from its bulk value (away from the vortex axis) to zero (on the vortex axis) over a distance of the order of the healing length. This distance is thus called the vortex core radius. In helium II, it is approximately 10^{-8} cm. We conclude that that although the velocity $\kappa/(2\pi r) \to \infty$ for $r \to 0$, there is no problem because in the same limit $\rho_s \to 0$.

Finally we compute the circulation around the vortex axis along a closed path C. Taking for C a circle of radius r we recover

$$\oint_C \mathbf{v}_s \cdot \mathbf{d}\boldsymbol{\ell} = \int_0^{2\pi} v_s r d\phi = \kappa, \tag{5.3.2}$$

as expected.

5.4 NLSE versus Euler

We have seen that the difference between the NLSE and the Euler equation is the quantum stress term. The natural question is thus in which sense a superfluid is similar to a classical inviscid Euler fluid.

Let D be the typical length scale of a problem. The ratio of the pressure term and the quantum stress term in the NLSE scales as $\hbar^2/(mE_0D^2)$, which is unity for $D \sim a_0$. We conclude that the quantum stress is important only at scales not larger than the healing length, $D \ll a_0$.

The quantum stress is indeed responsible for phenomena such as vortex nucleation, see Frish, Pomeau, and Rica (1992) and Winiecki and Adams (2000), and vortex reconnections, see Koplik and Levine (1993); these phenomena are outside the range of predictions of the classical Euler equations. Away from vortices, however, where the density is approximately constant, the quantum stress is zero, and the NLSE reduces to the Euler equation. Since the healing length is $a_0 \approx 10^{-8}$ cm and the typical vortex separation in quantum turbulence experiments is $\ell \approx 10^{-3}$ to 10^{-4} cm, there is a wide separation between the two scales. We conclude that, apart from relatively rare events such as vortex reconnections and nucleation, in most of the flow at most of the time the superfluid described by the NLSE is essentially a classical inviscid Euler fluid.

6 Two–fluid model with friction

6.1 Mutual friction

Quantised vortex lines interact with the phonons and rotons which make up the normal fluid, thus coupling the superfluid component with the normal fluid component, see Barenghi, Donnelly, and Vinen (1983). The coupling force $\mathbf{F}_{ns}$ is called mutual friction. It is proportional to the relative velocity between the two fluids, acting as a friction on each fluid. Thus, in the presence of quantised vorticity, the momentum conservation equations of Landau's two–fluid model become

$$\rho_n \left(\frac{\partial \mathbf{v}_n}{\partial t} + (\mathbf{v}_n \cdot \nabla)\mathbf{v}_n \right) = -\frac{\rho_n}{\rho}\nabla p - \rho_s s \nabla T, + \eta \nabla^2 \mathbf{v}_n + \mathbf{F}_{ns}, \tag{6.1.1}$$

$$\rho_s \left(\frac{\partial \mathbf{v}_s}{\partial t} + (\mathbf{v}_s \cdot \nabla)\mathbf{v}_s \right) = -\frac{\rho_s}{\rho}\nabla p + \rho_s s \nabla T - \mathbf{F}_{ns}. \tag{6.1.2}$$

6.2 Attenuation of second sound

Consider a vessel which contains helium II and rotates at constant angular velocity Ω. A second sound pulse or resonance which moves across helium suffers a bulk attenuation. What concerns us here is the extra attenuation which arises due to the presence of vortices, shown in Figure 6.2.1. This extra attenuation can be used to measure the density of vortex lines.

Following Hall and Vinen (1956), the mutual friction force is

$$\mathbf{F}_{ns} = \frac{B\rho_n\rho_s}{\rho}\hat{\mathbf{\Omega}} \times (\mathbf{\Omega} \times \mathbf{q}) + \frac{B'\rho_n\rho_s}{\rho}\mathbf{\Omega} \times \mathbf{q}, \tag{6.2.1}$$

where

$$\mathbf{q} = \mathbf{v}_n - \mathbf{v}_s, \tag{6.2.2}$$

and B and B' are temperature–dependent mutual friction coefficients which depend on the interaction of phonons and rotons with the quantised vortices. Substituting $\mathbf{q}$ and $\mathbf{F}$ into the Equation (6.1.1) and Equation (6.1.2), we obtain the following second sound wave equation:

$$\frac{d^2\mathbf{q}}{dt^2} + (2 - B')\mathbf{\Omega} \times \frac{d\mathbf{q}}{dt} - B\hat{\mathbf{\Omega}} \times (\mathbf{\Omega} \times \frac{d}{dt}\mathbf{q}) = c_2^2 \nabla(\nabla \cdot \mathbf{q}) \tag{6.2.3}$$

Let us assume that the second sound propagates in the x direction:

$$\mathbf{q} = (q_x, q_y, 0)e^{ikx - i\omega t}, \tag{6.2.4}$$

where k is the wavenumber and ω the angular frequency. In typical experimental conditions we have $\Omega/\omega \ll 1$, hence we obtain

$$k \approx \frac{1}{c_2}(\omega + i\frac{\Omega B}{2}). \tag{6.2.5}$$

The attenuation coefficient $\tilde{\alpha}$ is the imaginary part of k:

$$\tilde{\alpha} = \frac{B\Omega}{2c_2}. \tag{6.2.6}$$

In fact

$$\mathbf{q} = (q_x, q_y, 0)e^{-\tilde{\alpha}x}e^{i\omega(x/c_2 - t)}, \tag{6.2.7}$$

Note that angular velocity of rotation Ω is related to the vortex line density L via Feynman's rule, Equation (4.3.1), so, by measuring $\tilde{\alpha}$, we can recover the vortex line density.

It is therefore possible to perform an absolute measurement of the amount of vortex lines which are present in a turbulent flow. First the vessel is rotated, and the second sound signal is calibrated against the known vortex line density (number of vortices per unit area) $L = 2\Omega/\kappa$. Secondly, the vessel is stopped, the turbulence experiment is performed, and the second sound attenuation allows us to recover the vortex line density L (now to be interpreted as the vortex length per unit volume). Finally, it must be noticed that second sound is not attenuated by vortex lines which are parallel to the direction of propagation. If we assume that the turbulence is isotropic, only 2/3 of the vortices will attenuate the second sound wave.

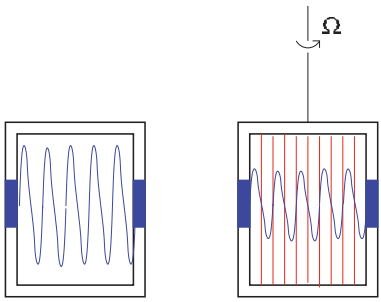

Figure 6.2.1. Left: second sound wave in a non–rotating vessel (no vortices). Right: second sound wave in the presence of vortices in a rotating vessel (vortices are present): note the reduced amplitude of the wave.

7 Vortex dynamics

7.1 The Biot–Savart law

The radius of the superfluid vortex core, approximately $a \approx 10^{-8}$ cm, is much smaller than any length scale of interest, so it is a good idea to approximate vortex lines as space curves of infinitesimal thickness. This approach was introduced by Schwarz (1985, 1998). The curves must be either closed loops or end at a boundary because a vortex cannot terminate in the middle of the flow.

Let $\mathbf{s} = \mathbf{s}(\xi)$ be the position of a point on such a curve, where ξ is the arc length. Following the classical theory of space–curves, we define the tangent $\hat{\mathbf{T}}$, normal $\hat{\mathbf{N}}$ and binormal $\hat{\mathbf{B}}$ unit vectors:

$$\mathbf{s}' = \frac{d\mathbf{s}}{d\xi} = \hat{\mathbf{T}}, \tag{7.1.1}$$

$$\frac{d\hat{\mathbf{T}}}{d\xi} = c\hat{\mathbf{N}}, \tag{7.1.2}$$

$$\hat{\mathbf{B}} = \hat{\mathbf{T}} \times \hat{\mathbf{N}}, \tag{7.1.3}$$

where $c = |\mathbf{s}''|$ is the curvature and $R = 1/c$ the local radius of curvature. The three vectors $\hat{\mathbf{T}}$, $\hat{\mathbf{N}}$ and $\hat{\mathbf{B}}$ form a right–handed system, as shown in Figure 7.1.1.

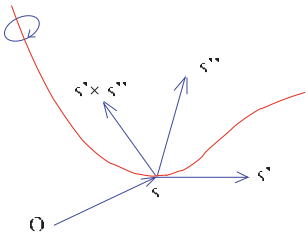

Figure 7.1.1.

The next step is to find the equation of motion of the vortex line. We start from classical definition of vorticity field $\boldsymbol{\omega}$ associated with a velocity field $\mathbf{v}$:

$$\boldsymbol{\omega} = \nabla \times \mathbf{v}. \tag{7.1.4}$$

Let us introduce the vector potential $\mathbf{v} = \nabla \times \mathbf{A}$; then $\mathbf{A}$ obeys the Poisson equation

$$\nabla^2 \mathbf{A} = -\boldsymbol{\omega}, \tag{7.1.5}$$

whose solution is

$$\mathbf{A}(\mathbf{x}) = \frac{1}{4\pi} \int \frac{\boldsymbol{\omega}(\mathbf{x}')d^3x'}{r}, \tag{7.1.6}$$

where $r = |\mathbf{x} - \mathbf{x}'|$. In our case the vorticity is formally concentrated on the vortex filament, $\boldsymbol{\omega}(\mathbf{x}')d^3x' = \kappa \mathbf{d}\boldsymbol{\ell}(\mathbf{x}')$, thus

$$\mathbf{A} = \frac{\kappa}{4\pi} \oint \frac{1}{r} \mathbf{d}\boldsymbol{\ell}', \tag{7.1.7}$$